Defense Nuclear Agency
Alexandria, VA 22310-3398

DNA-TR-89-20-V5

Target Area Studies
Volume V—An Analytical Model for Three-Dimensional Stabilized Plumes

Daniel Weihs
Richard D. Small
Pacific-Sierra Research Corporation
12340 Santa Monica Boulevard
Los Angeles, CA 90025-2587

September 1991

Technical Report

CONTRACT No. DNA 001-88-C-0119

DISCLAIMER NOTICE

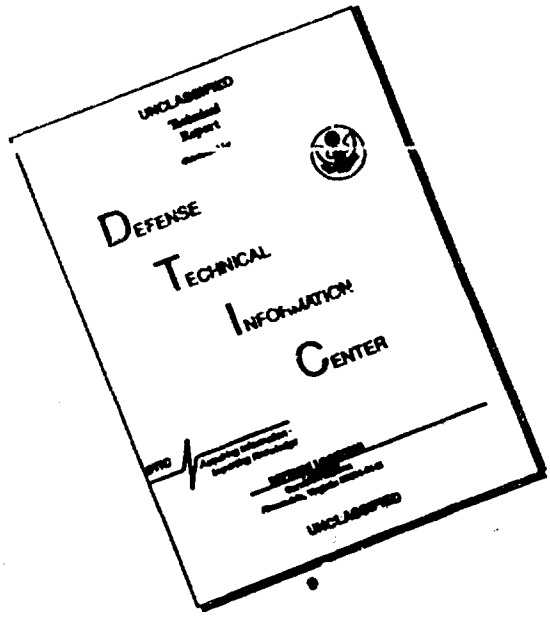

THIS DOCUMENT IS BEST QUALITY AVAILABLE. THE COPY FURNISHED TO DTIC CONTAINED A SIGNIFICANT NUMBER OF PAGES WHICH DO NOT REPRODUCE LEGIBLY.

Destroy this report when it is no longer needed. Do not return to sender.

PLEASE NOTIFY THE DEFENSE NUCLEAR AGENCY, ATTN: CSTI, 6801 TELEGRAPH ROAD, ALEXANDRIA, VA 22310-3398, IF YOUR ADDRESS IS INCORRECT, IF YOU WISH IT DELETED FROM THE DISTRIBUTION LIST, OR IF THE ADDRESSEE IS NO LONGER EMPLOYED BY YOUR ORGANIZATION.

REPORT DOCUMENTATION PAGE

Form Approved
OMB No. 0704-0188

1. AGENCY USE ONLY *(Leave blank)*	2. REPORT DATE	3. REPORT TYPE AND DATES COVERED
	910901	Technical 850519 - 881223

4. TITLE AND SUBTITLE
Target Area Studies
Volume V—An Analytical Model for
Three-Dimensional Stabilized Plumes

5. FUNDING NUMBERS
C - DNA 001-88-C-0119
PE - 62715H
PR - RM
TA - RA
WU - DH047780

6. AUTHOR(S)
Daniel Weihs and Richard D. Small

7. PERFORMING ORGANIZATION NAME(S) AND ADDRESS(ES)
Pacific-Sierra Research Corporation
12340 Santa Monica Boulevard
Los Angeles, CA 90025-2587

8. PERFORMING ORGANIZATION REPORT NUMBER
PSR Report 1842

9. SPONSORING/MONITORING AGENCY NAME(S) AND ADDRESS(ES)
Defense Nuclear Agency
6801 Telegraph Road
Alexandria, VA 22310-3398
RARP/Auton

10. SPONSORING/MONITORING AGENCY REPORT NUMBER
DNA-TR-89-20-V5

11. SUPPLEMENTARY NOTES
This work was sponsored by the Defense Nuclear Agency under RDT&E RMC Code B3500A 4662D RM RA 00001 25904D.

12a. DISTRIBUTION/AVAILABILITY STATEMENT
Approved for public release; distribution is unlimited.

12b. DISTRIBUTION CODE

13. ABSTRACT *(Maximum 200 words)*

We develop a simple analytical model to estimate the thickness of a smoke layer formed by a plume of a large area fire and to account for crosswinds. We take advantage of the dominant flow features in the upper part of the rising plume and in the smoke layer far from the plume to model the transition of a vertical flow to a horizontally spread thin smoke (or dust) layer. A one-dimensional approximation is used to model the buoyancy decay and plume overshoot. That solution is matched and combined with a solution based on the work required to establish our asymptotic horizontal smoke layer. The solution estimates the thickness of the spreading smoke layer in a quiescent atmosphere or in an ambient wind field.

14. SUBJECT TERMS		15. NUMBER OF PAGES
Smoke Layers Plumes	Large Fires	32
		16. PRICE CODE

17. SECURITY CLASSIFICATION OF REPORT	18. SECURITY CLASSIFICATION OF THIS PAGE	19. SECURITY CLASSIFICATION OF ABSTRACT	20. LIMITATION OF ABSTRACT
UNCLASSIFIED	UNCLASSIFIED	UNCLASSIFIED	SAR

CLASSIFIED BY:

N/A since Unclassified

DECLASSIFY ON:

N/A since Unclassified

SUMMARY

We develop a simple analytical model to estimate the thickness of a smoke layer formed by the plume of a large area fire and to account for crosswinds. We take advantage of the dominant flow features in the upper part of the rising plume and in the smoke layer far from the plume to model the transition of a vertical flow to a horizontally spread thin smoke (or dust) layer. A one-dimensional approximation is used to model the buoyancy decay and plume overshoot. That solution is matched and combined with a solution based on the work required to establish our asymptotic horizontal smoke layer. The solution estimates the thickness of the spreading smoke layer in a quiescent atmosphere or in an ambient wind field.

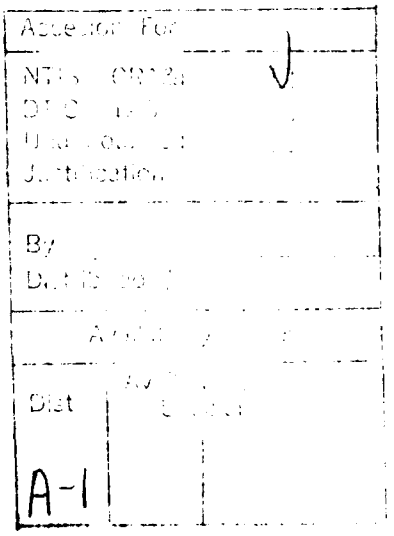

PREFACE

This report continues Pacific-Research Corporation's study of nuclear weapon fire effects. In this volume we develop a simple model to predict the stabilization altitude and thickness of smoke layers formed by large fires. Such smoke layers spread over large distances and can obscure large areas. The cloud altitude and thickness are inputs for meso- and global-scale environment calculations.

This research was supported by the Defense Nuclear Agency under contract DNA 001-88-C-0119 and was monitored by Dr. David Auton, RARP.

CONVERSION TABLE

Conversion factors for U.S. Customary to metric (SI) units of measurement

MULTIPLY → / TO GET ←	BY → / BY ←	TO GET / DIVIDE
angstrom	1.000 000 x E -10	meters (m)
atmosphere (normal)	1.013 25 x E +2	kilo pascal (kPa)
bar	1.000 000 x E +2	kilo pascal (kPa)
barn	1.000 000 x E -28	meter^2 (m^2)
British thermal unit (thermochemical)	1.054 350 x E +3	joule (J)
calorie (thermochemical)	4.184 000	joule (J)
cal (thermochemical)/cm^2	4.184 000 x E -2	mega joule/m^2 (MJ/m^2)
curie	3.700 000 x E +1	*giga becquerel (GBq)
degree (angle)	1.745 329 x E -2	radian(rad)
degree Fahrenheit	$t_K = (t°f + 459.67)/1.8$	degree kelvin (K)
electron volt	1.602 19 x E -19	joule (J)
erg	1.000 000 x E -7	joule (J)
erg/second	1.000 000 x E -7	watt (W)
foot	3.048 000 x E -1	meter (m)
foot-pound-force	1.355 818	joule (J)
gallon (U.S. liquid)	3.785 412 x E -3	meter^3 (m^3)
inch	2.540 000 x E -2	meter (m)
jerk	1.000 000 x E +9	joule (J)
joule/kilogram (J/kg) (radiation dose absorbed)	1.000 000	Gray (Gy)
kilotons	4.183	terajoules
kip (1000 lbf)	4.448 222 x E +3	newton (N)
kip/in^2 (ksi)	6.894 757 E +3	kilo pascal (kPa)
ktap	1.000 000 x E +2	newton-second/m^2 (N-s/m^2)
micron	1.000 000 x E -6	meter (m)
mil	2.540 000 x E -5	meter (m)
mile (international)	1.609 344 x E +3	meter (m)
ounce	2.834 952 x E -2	kilogram (kg)
pound-force (lbs avoirdupois)	4.448 222	newton (N)
pound-force inch	1.129 848 x E -1	newton-meter (N m)
pound-force/inch	1.751 268 x E +2	newton/meter (N/m)
pound-force/foot^2	4.788 026 x E -2	kilo pascal (kPa)
pound-force/inch^2 (psi)	6.894 757	kilo pascal (kPa)
pound-mass (lbm avoirdupois)	4.535 924 x E -1	kilogram (kg)
pound-mass-foot^2 (moment of inertia)	4.214 011 x E -2	kilogram-meter^2 (kg m^2)
pound-mass/foot^3	1.601 846 x E +1	kilogram/meter^3 (kg/m^3)
rad (radiation dose absorbed)	1.000 000 x E -2	**Gray (Gy)
roentgen	2.579 760 x E -4	coulomb/kilogram (C/kg)
shake	1.000 000 x E -8	second (s)
slug	1.459 390 x E +1	kilogram (k)
torr (mm Hg, 0°C)	1.333 22 x E -1	kilo pascal (kPa)

*The becquerel (Bq) is the SI unit of radioactivity: 1 Bq = 1 event/s.

**The Gray (Gy) is the SI unit of absorbed radiation.

TABLE OF CONTENTS

LIST OF ILLUSTRATIONS

SECTION 1
INTRODUCTION

The spread of smoke over regional scales depends on the initial smoke injection and the temperature and wind structure of the atmosphere. Although the transition from a vertical plume flow to a horizontal cloud is three-dimensional, separately, the spread and the injection can be approximated as two-dimensional flows. Regional particulate cloud movements are often in thin layers with only slow changes normal to the principal flow direction [Westphal, et al., 1988]. Similarly, large fire plume motions are principally vertical and two-dimensional (axisymmetric) [Small and Larson, 1985; Small and Heikes, 1988]. A similar division of flows also occurs when the dust plume following a rising fireball is sheared at the stabilization altitude.

Plumes formed by nuclear weapon fires [Small, 1989] can have diameters comparable to the atmospheric scale height. The plume motion is thus a significant perturbation to the atmosphere. Gravity waves which propagate long distances are formed by dynamical processes in the fire inflow region or by the oscillation of the plume about its neutral buoyancy level in the upper atmosphere [Heikes and Small, 1990a]. Large fire plumes can penetrate high into the atmosphere; their rise limited mostly by gradients in temperature and winds. Because nuclear weapon fires can cover several hundred square kilometers and plume diameters can be roughly 10 km or greater, ambient winds do not greatly influence the plume motion over most of its rise. However, near the top of the plume, the buoyancy is reduced and the motion slows, upper level winds bend the column and the plume is sheared into thin clouds that are advected away from the target area. The thickness of the spreading cloud can be calculated [Small and Heikes, 1989; Heikes and Small, 1990a] in quiescent atmospheres. Two-dimensional or axisymmetric hydrocode solutions can calculate the plume rise, overshoot, and settling at the neutral buoyancy level. Such solutions, however, do not account for crosswinds; three-

dimensional hydrocodes are required and only a few solutions have been developed [Cotton, 1985; Bradley et al., 1988]. In those solutions, the resolution is fairly coarse and the cloud thickness far from the plume is only estimated.

An alternative to three-dimensional code solutions uses modifications of the Morton et al. [1956] plume similarity solution to account for cross-winds [Briggs, 1975; Manins, 1985]. Such solutions are valid for asymptotically slender plumes in which the buoyancy is diffused by entrainment of ambient air. For nuclear weapon fire plumes--or even large prescribed fires [Heikes and Small, 1990a]--the plume is too thick for entrainment at the edge to diffuse the buoyancy or momentum. Similarity type solutions have been applied to plumes from industrial or utility smoke stacks. They are not applicable for nuclear weapon smoke or dust plumes.

In this report, we develop a simple two-dimensional model to estimate the thickness of the smoke (or dust) cloud far from the plume and to account for crosswinds. We take advantage of the dominant flow features in the rising plume and far field to model the transition of a vertical flow to a horizontally spreading thin smoke (dust) layer. A one-dimensional approximation is used to model the buoyancy decay and plume overshoot. That solution is matched and combined with a solution based on the work required to establish a asymptotic horizontal smoke layer. The solution while approximate estimates the thickness of clouds that merge (for multiple plumes) and spread regionally.

SECTION 2
ANALYSIS

In the upper portion of the plume region, the combustion products and entrained air have been moving upwards for a time of order z/W where the height z is of order 1000 m and the average vertical velocity W is of order 10 m/s. Even for low turbulence levels, the plume is well mixed and in approximate thermal equilibrium. The density deficit (buoyancy), pressure, and the velocity are thus well defined, continuous functions of position.

The full flowfield describing the formation of a capping cloud is subtle, involving the interaction of small temperature, density and pressure differences within and external to the plume. However, by breaking the flowfield into zones, most of the important features of the upper plume can be described by simple models. These include the bending of the plume axis by crosswinds, establishing the maximum height obtained by the combustion products, and determining the shape and thickness of the outward spreading smoke layer as a function of distance from the plume center. The altitude and thickness of the initial layer is the initial condition for calculating the mesoscale spread of smoke. The cloud's position relative to the tropopause influences the rate of scavenging. At low altitudes precipitation enhances particle removal while in the stratosphere removal is slow.

The fire induced flowfield can be described by six zones, each of which is dominated by different physical mechanisms. Simple equation sets can be separately formulated for each zone, and the results patched. The zones are (see Fig. 1):

1. **Inflow layer.** Approximated by a sink-like flowfield [Weihs and Small, 1986]. In this zone air moves at low (incompressible) speeds close to ground level. The inflow (fire winds) provides oxygen for the fire; it is driven by the pressure deficit in the burning zone. Here $r > R_f$, $z < H_o$.

2. **The flame and combustion zone.** Defined as a cylindrical volume of radius R_f and height H_f in which exothermic reactions take place; combustibles and air are turned into hot buoyant plume gases.

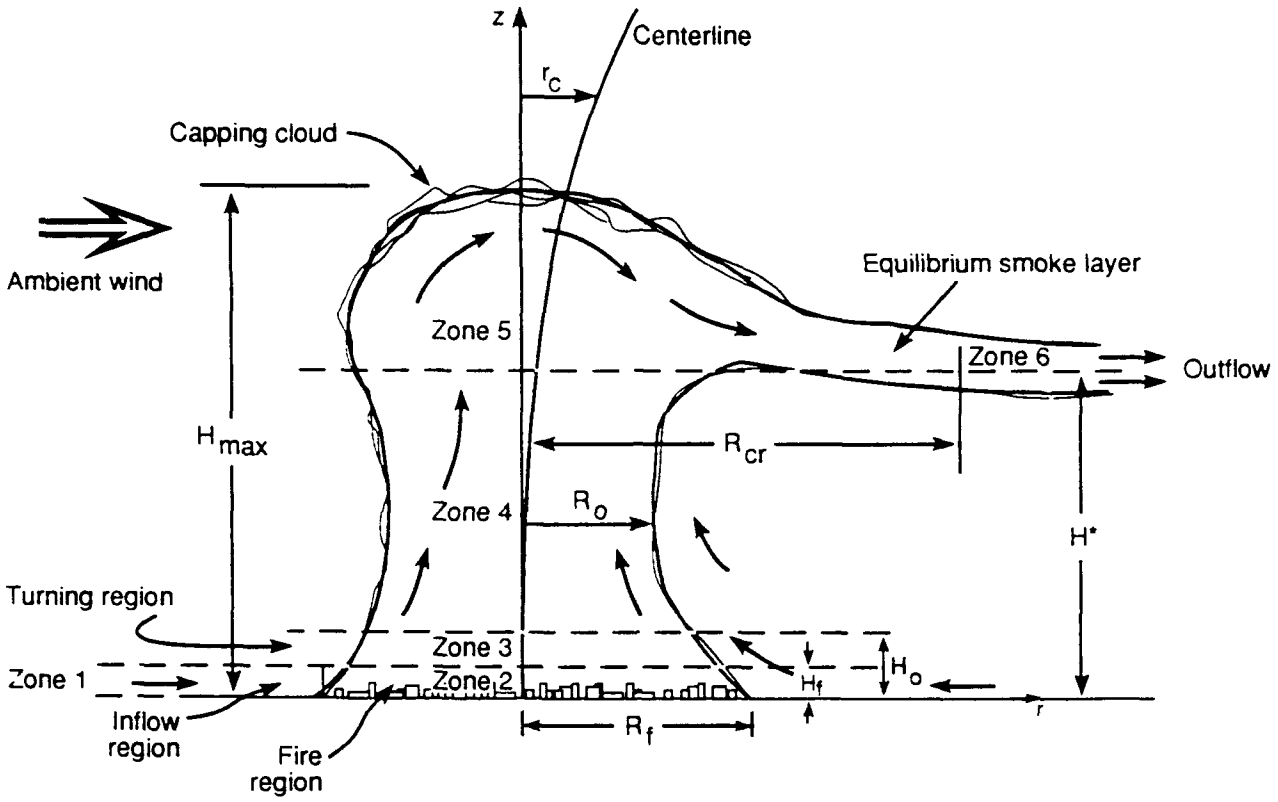

Figure 1. Schematic representation identifying principal flow regions of axisymmetric plume driven by a large area fire.

3. **Turning region.** Here the radial inflow reduces the diameter of the upward moving plume. Initially, the contraction angle is quite acute. The slope is reduced at higher elevations as the plume contracts, accelerating the vertical motion, while inflow is reduced. The vertical bounds of zone 3 are $H_f < z < H_o$. Buoyance is initially high, and heat loss by radiation is a significant factor.

4. **Central column.** This is a major part of the convection column; the flow is essentially parallel, moves upwards and can be approximated as one-dimensional. Temperature differences and buoyant forces are small. Shear at the column perimeter affects only a relatively thin boundary layer. At the upper end of zone 4, the plume density is equal to that of the atmosphere, and crosswinds start shearing the plume.

5. **Capping cloud.** In this region the plume density is essentially constant and greater than the surrounding air. The upward momentum causes the plume to rise further and finally fall back, while crosswinds advect it downstream. It then spreads horizontally. The flow in this zone is intrinsically

three-dimensional, ending at a distance where the vertical component is much smaller than the horizontal one. This defines a critical radius (R_{cr}).

6. **Equilibrium cloud layer.** This is a region of purely horizontal flow, at a height H^* . This zone is an annular disk of radius $r > R_{cr}$ with slowly varying width (the final cloud layer thickness) distorted by ambient crosswinds.

2.1 CENTRAL COLUMN ANALYSIS.

We first consider the flow in zone 4 without ambient winds. This analysis is the starting point for including crosswinds and estimating the maximum overshoot height H_{max} (top of zone 5).

Zone 4 is characterized by weak, decreasing buoyancy and negligible entrainment. Initial conditions at H_o include the vertical velocity and the temperature excess. These are obtained from either analytic solutions [Small and Larson, 1985] or from hydrocode simulations of the fire zone [Bacon et al., 1987; Penner et al., 1986; Small and Heikes, 1989; Heikes and Small, 1990a,b]. Maximum speeds are generally O[10] m/s and the temperature excess is small, usually less than 10 K. The largest values of both are at the plume axis (this may be an artifact of the radial symmetry, although in large experimental fires [Radke, 1990], the plume top is generally near the fire center).

To establish the dominant flow features, we make several assumptions that simplify the formulation. We assume steady flow. The analysis is thus valid after the initial ignition-fire plume formation transients are over and almost to burnout. The initial transients generally last 5 to 20 minutes. Typical fires last 1 to 4 h [Small, 1989] so that over 80 percent of the fire duration is covered by the present analysis.

The plume is assumed mostly air with properties of an ideal gas. Most fires burn with excess air and the combustion products generally comprise less than several percent of the total, even if perfect combustion is achieved (stoichiometric ratios for most prevalent combustibles are around 15:1). The amount of water added by combustion products is usually small relative to entrained ambient humidity, except in particularly arid areas [Small and Heikes, 1987].

Heat transfer between the plume and surroundings is neglected. Zone 3 may have significant heat loss due to radiation [Murgai, 1962; Smith, 1967]. Above that region, temperature differences are small, and adiabatic or pseudo-adiabatic flow is assumed in zones 4, 5, and 6.

Mass transfer between the plume and the surroundings is negligible. This is equivalent to assuming that all entrainment takes place in the lower zones, and that the plume mass flux in zone 4 changes only slightly. Thus, the limiting streamlines (recalling the assumption of steady flow) defined at the lowest plane of zone 4 outlines the plume trajectory.

The structure of the external atmosphere is not strongly influenced by the presence of the plume, and the boundary conditions for external pressure, density, and temperature are independent of time and fire parameters.

The altitude H^* defining the equilibrium height of the cloud, as well as the upper end of zone 4, and the vertical velocity (W^*) at the altitude is obtained from one dimensional flow considerations. The equation of continuity now reads simply

$$\rho w A = \text{Const} \quad , \tag{1}$$

where A is fixed, and input conditions at H_o obtained from a separate analysis or numerical results [Small et al., 1988]. Equation (1) is rewritten as

$$W^* = \frac{\rho_o}{\rho^*} W_o \quad . \tag{2}$$

Equation (2) provides the value W^* once the density equation is found. The density changes in the plume are adiabatic so that

$$\left[\frac{P(z)}{\rho(z)}\right]^\gamma = \left[\frac{P_o}{\rho_o}\right]^\gamma = K \quad . \tag{3}$$

The ambient atmosphere has a lapse rate dependent on time of day, season, and humidity. This requires an independent set of functions to describe the altitude variation of pressure and density. Additional information is required to find the equilibrium density, that is the density where both Eq. (3) and the specific meteorology give the same values for both pressure and density. This density then defines the equilibrium height H^*, and by Eq. (2) the velocity W^*. The density distribution is affected by water vapor. The main effect is due to moisture (ambient humidity) entrained by the firewinds (water produced as a product of combustion is small compared to the entrained moisture). For the following calculations, we use a standard relative humidity model [Manabe and Wetherall, 1967]

$$RH(z) = \frac{RH(0)}{0.98}\left[\frac{P(z)}{P(o)} - 0.02\right] \quad .$$

The humidity at the bottom of zone 4 is the average humidity over the height range $0 < z < 1000m$. The ambient humidity produces saturation (except in very arid cases) as the ambient temperature falls and the dew-point is crossed. Most of the condensation occurs within zone 4. The latent heat released reduces the density which effectively increases K in Eq. (3).

2.2 ANALYSIS OF CAPPING CLOUD REGION.

This same model is also used to calculate the maximum height obtained by the plume (H_{max}). This calculation assumes [Turner, 1973] that density is constant in overshoot regions such as zone 5. The maximum height is achieved by the central streamline so that a one-dimensional calculation again is sufficient. For these assumptions, the momentum equation in the vertical direction reduces to

$$\frac{dw^2}{dz} = 2g\left[\frac{\rho}{\rho_a(z)} - 1\right] \quad , \qquad (4)$$

where $\rho_a(z)$ is the ambient density. Integrating Eq. (4) over z gives the vertical velocity distribution as a function of ambient density and the initial profile from zone 3.

Results of these computations for a 7 km diameter fire and average heat addition rate of 100 KW/m^3 are shown in Figs. 2 and 3. Input conditions at z = 1000 m are ΔT = 10 K and W_o = 10 m/s [Small and Heikes, 1988]. The standard day absolute humidity is nominally 7.5 g H_2O/kg dry air. For this fire, the condensation height was ~2500 m, the equilibrium smoke layer height ~11 km, and the maximum plume height about 15 km. The comparison of predicted cloud altitudes in Fig. 2 shows that the present approximation satisfactorily estimates the maximum altitudes within the range and spread of current hydrocode results.

2.3 PLUME RISE IN CROSSWIND.

Next, we consider the plume rise in zone 4 when subjected to ambient crosswinds. Annually averaged wind velocities as a function of height above sea level are given in Fig. 4. The "standard" profile averages wind profiles used by Penner et al., [1986] and Scoggins and Vaughan [1962]. The latter windspeeds are O[10 m/s] (comparable to the upflow speeds in zone 4).

To enable a semi-analytic solution for the plume deflection by such crosswinds, several simplifying steps are made. We assume that plume horizontal cross-sections stay round and that the rising plume gases do not mix with the ambient air, i.e., the plume boundary is a streamtube. Each horizontal cross-section is assumed to be displaced relative to its vertical neighbors under the influence of the wind at its height. The resulting bending of the plume can thus be visualized as a series of disks pushed sideways by a force varying with height.

There are three possible contributions to the horizontal force. These are the aerodynamic drag force between wind and plume, the centrifugal force resulting from plume bending, and the Coriolis force which results from the angle between the vertical plume and the Earth's rotation vector (complementary angle to latitude). The Coriolis acceleration is

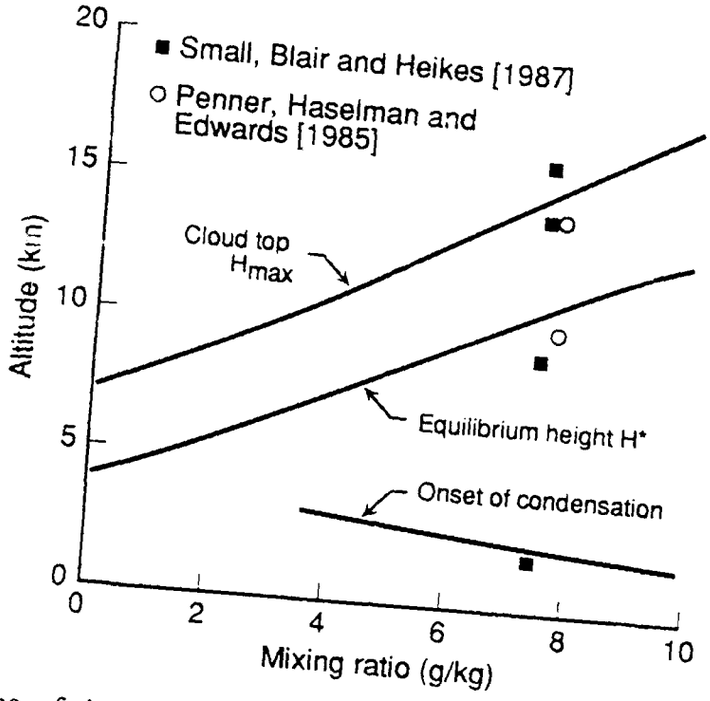

Figure 2. Influence of initial mixing ratio on altitude of cloud top, equilibrium smoke layer, and onset of condensation. (U.S. standard atmosphere assumed. Curves represent present results.)

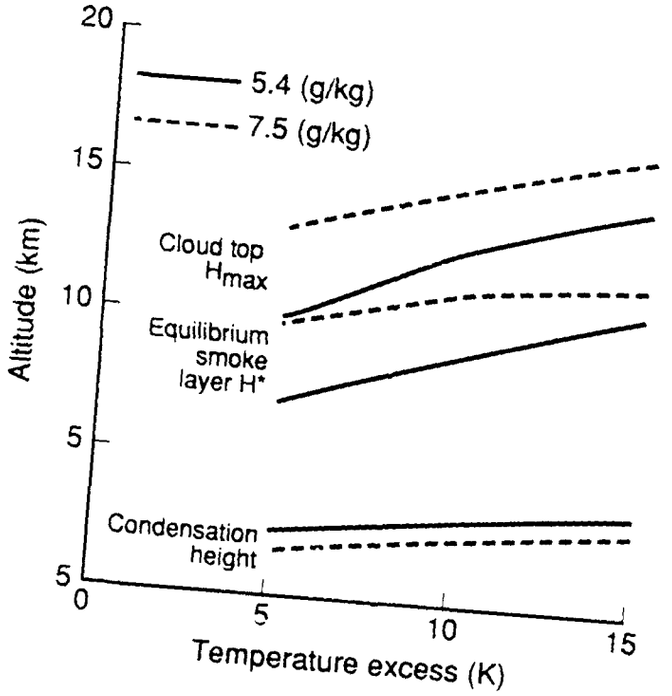

Figure 3. Cloud and smoke layer altitudes for prescribed initial temperature excess at 1 km. Lower level humidity influences cloud height.

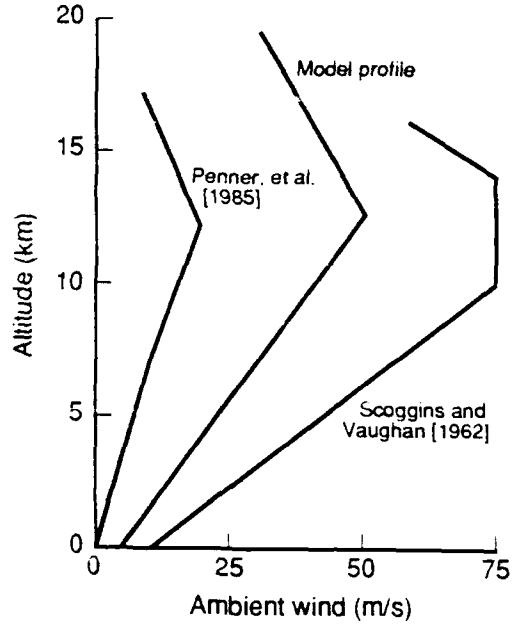

Figure 4. Model velocity profiles representing average atmospheric wind conditions.

$$a = 2\Omega w \cos\phi \quad , \tag{5}$$

where $\Omega = 0.0073$ rad/s is the Earth's angular velocity, w is the vertical velocity of the plume and ϕ is the geographic latitude. We directly obtain the horizontal displacement of the plume centerline as a function of fluid particle "residence time" in zone 4, $\tau_c = \Delta H/w$. This is

$$\Delta x = a_c \tau_c^2/2 = \Omega (\Delta H/w)^2/2 \quad , \tag{6}$$

where $\Delta H = 15000$ m, and $100 > W > 20$ m/s, so that $\tau_c < 100$ s, and

$$\Delta x < 100 \text{ m} \quad , \tag{7}$$

i.e., much smaller than the other effects, as we shall demonstrate. We therefore neglect the displacement caused by the Coriolis effect in the following analysis.

The other two forces are the drag on the plume (the pushing force) and the centrifugal force resulting from the plume bending. These are equal and opposite, in the direction normal to the curved plume. The drag force per unit plume length is

$$dD = \rho_a V_w^2 \cos^2\theta \cdot b C_d \, dz \quad , \tag{8}$$

where ρ_a is the ambient air density, V_w is the windspeed, θ is the local angle, b is plume radius, and C_d is a drag coefficient. The centrifugal force obtained in the curved plume is

$$dF = m\left(\frac{dU_t}{dz}\right) dz = \rho_p U_t^2 \pi b^2 \frac{d\theta}{dz} dz \quad , \tag{9}$$

where ρ_p is the plume density, U_t is the total (including both vertical and horizontal components) of the velocity and $d\theta/dz$ is the local change of plume angle.

From Eqs. (9) and (2), we obtain

$$\frac{1}{\cos^2\theta} \frac{d\theta}{dz} = \frac{\rho_a}{\rho_p} \left(\frac{V_w}{U_t}\right)^2 \frac{C_d}{\pi b} \quad , \tag{10}$$

which is integrated to obtain the angular deflection of the rising plume as a function of height. Additional integration yields the horizontal motion of the plume centerline. A parametric study of plume centerline drift for the nominal 7 km fire is presented in Fig. 5. Three values are chosen for the drag coefficient. The highest value (0.7) is that of a solid, unmoving cylinder in high Reynolds number, fully turbulent flow. The plume boundary is not solid, so that the crosswind flow will cause some parallel motion in

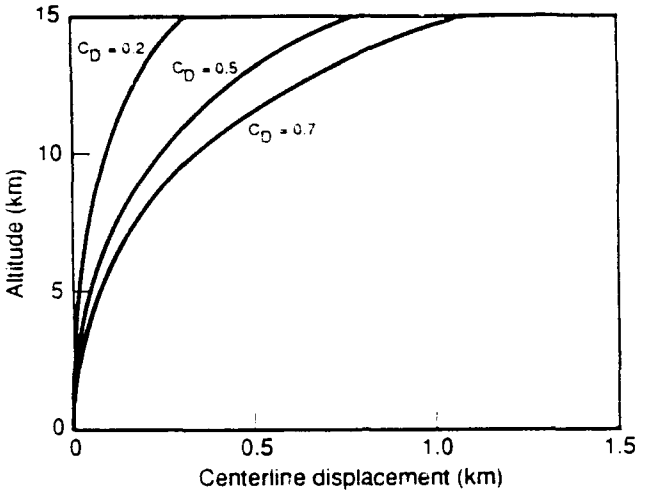

Figure 5. Plume centerline as a function of drag coefficient: 7 km radius fire; initial humidity ratio of 7.5 g/kg.

the plume reducing the drag. Thus, a realistic value for C_d is within the range described. Even for the lowest drag coefficient value, the displacement over 12 km is more than 200 m, i.e., more than twice the predicted upper limit of Coriolis driven motion (even neglecting the countering effect of centrifugal forces produced by this additional curvature). Neglecting the Coriolis force is thus justified a *posteriori*. The effects of fire radius are shown in Fig. 6 where the results collapsed onto a single curve when plotted against the product of the centerline displacement (r_c) and the fire radius R_f. This allows extrapolation to other fire sizes.

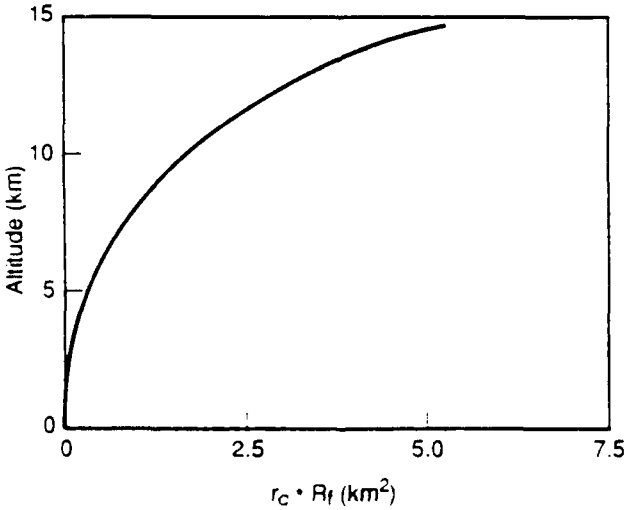

Figure 6. Plume centerline path for model wind field, w = 7.5 g/kg and C_d = 0.5

SECTION 3
THE EQUILIBRIUM SMOKE LAYER

Next, we examine zone 6 (see Fig. 1) and estimate the far field cloud layer thickness. The estimate is independent of the momentum, but depends on the mass and energy in the turned plume. The upward moving plume starts to turn at an altitude H^* where the plume density (now constant) exactly equals the density of the undisturbed atmosphere.

At this altitude, the plume is neutrally buoyant and has upward momentum only. As a result, a height overshoot or capping cloud develops (see Fig. 1). This is a local effect; the superelevated part of the plume has a radius of the order of the plume radius. We concentrate on determining the thickness and spread of a flat layer beyond the turning portion (zone 6), first in a quiescent atmosphere, and then accounting for crosswinds.

3.1 SMOKE LAYER THICKNESS WITH NO CROSSWIND.

The overturning process in zone 5 mixes the plume gases resulting in "top hat" profiles of the vertical velocity and the state variables. The mass flux in the rising part of the plume is:

$$\dot{M} = \rho_6 \, \pi \xi^2 \, R_f^2 \, W \quad , \tag{11}$$

where $\rho_6 = \rho_4$ is the plume density, $R_o = \xi R_f$ is the plume radius and W the speed. This, in turn, is equal to the flow at the perimeter of the layer, i.e.,

$$\dot{M} = \rho_6 \, 2\pi RTU \quad , \tag{12}$$

where T is the thickness (at the perimeter of the layer), U is the speed in the radial direction, and R is the radius. From Eqs. (11) and (12),

$$T = \frac{R_o^2 W}{2UR} \quad , \tag{13}$$

where for steady flow, both U and T are functions of the radial distance r only. The energy input per unit time is

$$\dot{E} = \dot{M} \frac{W^2}{2} \quad , \tag{14}$$

as the potential energy is now zero relative to the surroundings (no density difference). The rate of energy transported at cross section R is

$$\dot{E} = \dot{M} \frac{U^2}{2} + \dot{M}g \frac{T}{2} \quad . \tag{15}$$

The second term represents the energy required to maintain the layer of smoke at a given height. This energy is calculated by assuming that the layer centered at height H_o is compressed by the plume outflow. For a linearly decreasing density atmosphere, the change in volume of the lower column is, per unit radial distance

$$\Delta v = \frac{T}{2} \pi R^2 \quad . \tag{16}$$

The pressure applied per unit radial distance is obtained by dividing the plume weight produced per unit time by the area, i.e.,

$$p_a = \frac{\dot{M}g}{\pi R^2} \quad . \tag{17}$$

The work used for compression of the lower column is, per unit time from Eqs. (16) and (17)

$$P_a \, \Delta v = \dot{M} g \, \frac{T}{2} \quad . \tag{18}$$

Equating energies and assuming negligible viscous interactions (dissipation) we have

$$U^2 + g \, T = W^2 \quad , \tag{19}$$

Substituting Eq. (13) into Eq. (19),

$$U^3 - W^2 U + g \, \frac{W R_o^2}{2R} = 0 \quad . \tag{20}$$

One can obtain U(R) from Eq. (20) and then, using Eq. (13) solve for T(R) i.e., the layer speed and thus the thickness are functions of height and distance. Once T(R) is determined, one can generalize this solution to take crosswinds into account, this being the equivalent of having a source in an oncoming flow.

Equation (19) is a third degree equation in U which has one of three real solutions: 1) a negative radial velocity asymptotically approaching the value of (-W) as $R \to \infty$; 2) a pair of solutions that become real (and thus of practical interest) only if $R > R_{cr}$ where R_{cr} is larger than the original stem radius R_o (obtained at Z_o the lower edge of zone 4). At $R = R_{cr}$ these two solution branches have a common value of U, one growing asymptotically to the finite value $U - W_o$ as $R \to \infty$, the other tending to vanishingly small velocities for $R \to \infty$ (see Fig. 7).

The only physically reasonable solution is the third one with an asymptotically decreasing speed and a finite layer thickness at a large distance. The fact that this solution only occurs when $R > R_{cr}$ is compatible with the definition of zone 6 annular (i.e., the domain $R < R_{cr}$ is not included). The first solution requires inflow that is not consistent with a steady state flow. The second solution results in a vanishing thin layer in which viscous and mixing effects (which were neglected) would become dominant. The third solution results in

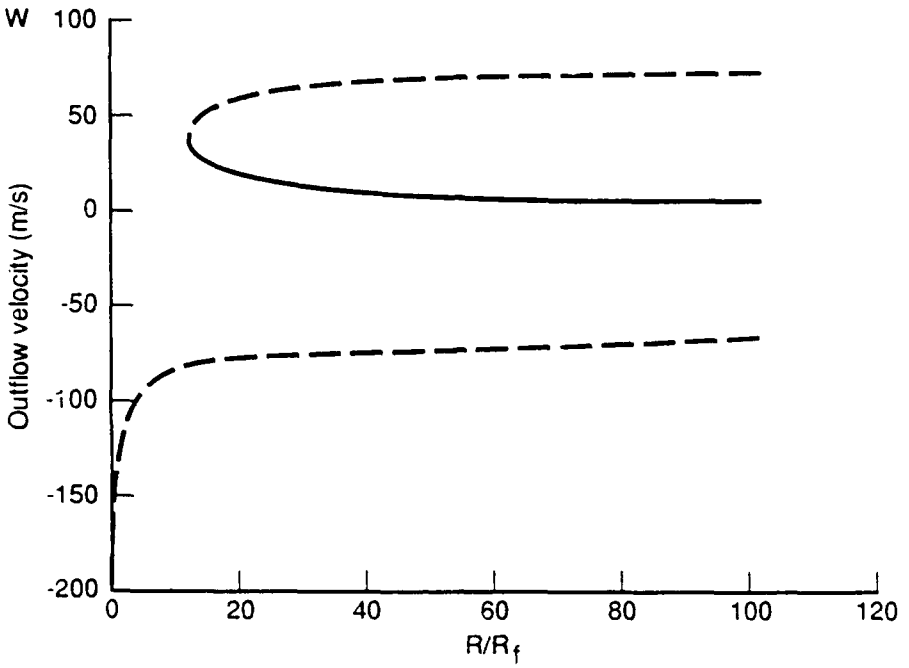

Figure 7. Solution branches for outflow layer velocity. Solid curve is the only physically valid solution (R_f = 7 km, W_{max} = 70 m/s).

a relatively thick layer in which edge effects are small. An asymptotic cloud thickness (see Fig. 8) of around 500 m is obtained for cloud radii of 100 km. The third physically significant solution has a domain of existence $R > R_{cr}$. The critical radius which defines the inner limit of the horizontal spreading zone is calculated as a function of the initial radius $R_o = \xi R_f$ and vertical velocity W. Figure 9 shows the value of the quantity R_{cr}/R_o^2. The value of the radial velocity U at the critical radius also appears in Fig. 9. Both velocities are linear functions of the parameter R_{cr}/R_o^2 for a wide range of upward velocities.

3.2 LAYER THICKNESS WITH CROSSWIND.

Numerical solutions for large fire plumes [Bacon et al., 1987; Penner et al., 1986; Small and Heikes, 1989] show rapidly decelerating vertical motions as the buoyancy decreases and eventually turns negative. Thus, even in a constant ambient wind, the plume tilts or shears more at the higher altitudes. This has been observed, for example, in the Canadian experimental fires [Heikes and Small,

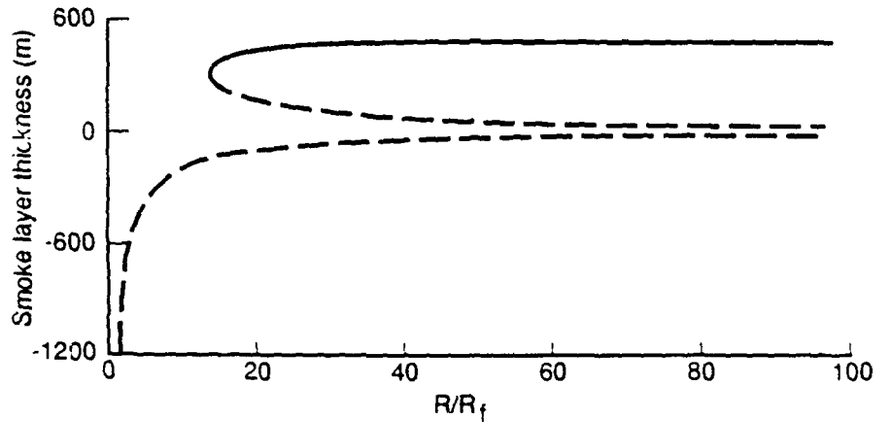

Figure 8. Solution branches for outflow layer thickness. Solid curve is the physically meaningful solution (R_f = 7 km, W_{max} = 70 m/s).

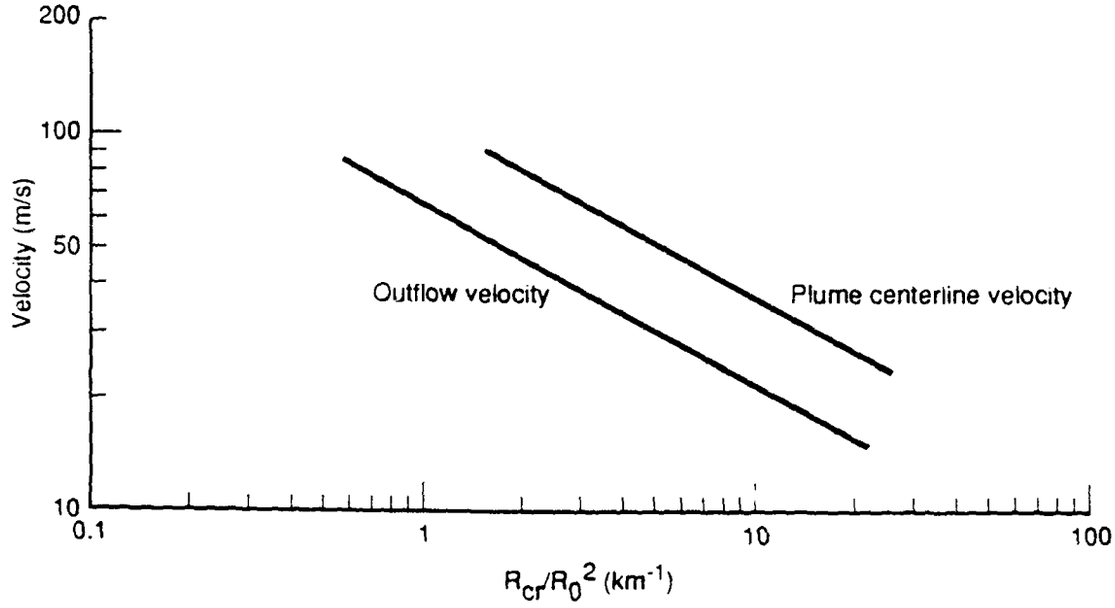

Figure 9. Outflow velocity at critical radius as a function of plume centerline velocity.

1990b]. The curving of the plume centerline is accentuated by the fact that windspeeds usually increase with altitude (see Fig. 4). The rising part is in principle described by circular cross sections in an obliquely curved plume. The local angle to the vertical is the ratio of average vertical velocity to horizontal velocity.

An additional process takes place at the top of the cloud layer. Since this layer is produced by an overshoot of the plume gases, the gases reach an altitude where their vertical velocity is vanishingly small before falling back and spreading out radially. With no external wind, this occurs on the outside of the ascending plume. Here, however, the windward part is blown towards the plume center and is shifted sideways and downstream.

When the smoke layer reaches its equilibrium height, the spread can be approximated by a simple two dimensional radial source flow. The flow is deflected by the wind into an elongated shape, calculated simply by superimposing the stream function representing the ambient wind which is [Milne-Thompson, 1968]

$$\psi_w = V_w z \tag{21}$$

on a source stream function

$$\psi_s = U_{cr} R_{cr} \theta \quad , \tag{22}$$

where θ is the circumforential coordinate. Since viscous forces are neglected, the combined stream function is

$$\psi = \psi_w + \psi_s \quad . \tag{23}$$

The cloud shape is thus a Rankine profile of finite length, obtained by plotting the curve $\psi = 0$ (see Fig. 10). The length of the Rankine wake (X_L in Fig. 10) is a function of the time elapsed since the plume started spreading. By conservation of mass using the layer thickness, the relation between the time elapsed since plume inception (Δt) and

the plume length is obtained. Figure 10 shows nondimensional wake length

$$X_2' = \frac{X_2}{r_{cr}} \frac{V_w}{U_{cr}} \tag{24}$$

as a function of the nondimensional layer area written as

$$S' = \pi \frac{w\Delta t}{T} \left(\frac{r_{eq}}{r_{cr}}\right)^2 \left(\frac{V_w}{U}\right)^2 . \tag{25}$$

For a given fire, S′ is proportional to the time elapsed and the length of the layer grows almost linearly with time, as expected.

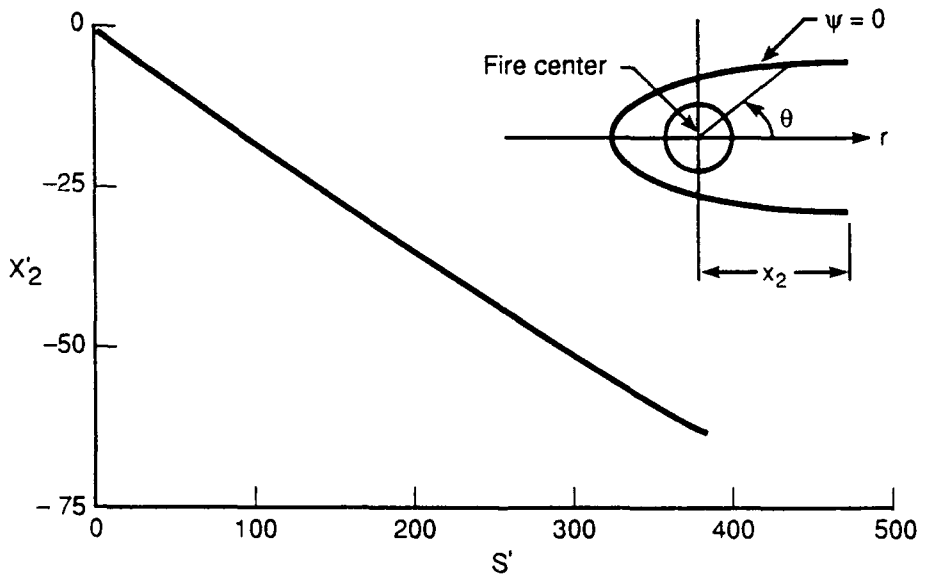

Figure 10. Nondimensional length of outflow layer as a function of the nondimensional layer area.

SECTION 4
CONCLUSIONS

We have shown that the maximum plume rise, altitude of the outflow smoke layer, and cloud spread rate (outflow velocity) while functions of the prescribed forcing, can be simply estimated. Although cloud heights were estimated for large area fires, a similar analysis could be developed for nuclear dust clouds.

The outflow layer, or mesoscale smoke cloud altitude and spread rate are determined by patching one-dimensional plume and equilibrium layer solutions through an energy formulation. The effects of crosswind are then accounted for by constructing a source function for the spreading plume and superimposing the ambient winds. The solutions, although approximate, provide rapid and reasonably accurate estimates of the smoke cloud height and the spreading cloud thickness. Such solutions could be used in evaluating mesoscale spread of smoke or dust layers and obscurations resulting from multiple nuclear bursts.

SECTION 5
LIST OF REFERENCES

Bacon, D. P., R. A. Sarma, and F. H. Proctor, *Smoke Injection Into the Atmosphere from Large Area Fires*, Science Applications International Corporation, McLean, VA, Report 86/1922, March 1987.

Bradley, M, K. R. Peterson, and D. J. Rodriguez, *Three Dimensional Numerical Modeling of Smoke Injection From Larger Fires in the Early Post-Nuclear-Exchange Environment*, UCRL-99562, Lawrence Livermore National Laboratory, Livermore, CA., November 1988.

Briggs, G. A., "Lectures on Air Pollution and Environmental Impact Analyses," *American Meteorological Society*, Boston, MA, pp. 59-111, 1975.

Cotton, W. R., "Atmosphere Convection and Nuclear Winter," *American Scientist*, Vol. 73, pp. 275-280, 1985.

Heikes, K. E., and R. D. Small, "Smoke Injection by Real Fires," *Proceedings of the Smoke/Obscurants Symposium XIV*, Laurel, MD, 1990a, in press.

Heikes, K. E., and R. D. Small, "Area Fire and Plume Behavior," in Heat and Mass Transfer in Frost and Ice Packed Beds, and Environmental Discharges, HTD-Vol. 139, *American Society of Mechanical Engineers*, June 1990b, pp. 135-141.

Manabe, S., and R. Wetherald, "Thermal Equilibrium of the Atmosphere with a Given DIstribution of Relative Humidity," *J. Atmospheric Sciences*, Vol. 24, No. 3, 1967.

Manins, P. C., "Cloud Height and Stratospheric Injections Resulting from a Thermonuclear War," *Atmospheric Environment*, Vol. 19, pp. 1245-1255, 1985.

Milne-Thompson, *Theoretical Hydrodynamics*, MacMillan, London, UK, 1968.

Morton, B. R., G. I. Taylor, and J. S. Turner, "Turbulent Gravitational Convection from Maintained and Instantaneous Sources," *Proceedings of the Royal Society*, Series A, Vol. 234, pp. 1-23, 1956.

Murgai, M. P., "Radiative Transfer Effects in Natural Convection Above Fires," *J. of Fluid Mechanics*, Vol. 12, pp. 441-448, 1962.

Penner, J. E., L. C. Haselman, and L. L. Edwards, "Smoke Plume Distribution Above Large Scale Fires: Implications for Simulations of Nuclear Winter," *J. Climate and Applied Meteorology*, Vol. 25, pp. 1434-1444, 1986.

Radke, L., et al., *Airborne Observations of Biomass Fires*, University of Washington, March 1990.

Scoggins, J. R., and W. W. Vaughan, *Cape Canaveral Wind and Shear Data (1 through 80 km) for Use in Vehicle Design and Performance Studies*, NASA Technical Note D-1274, 1962.

Small, R. D., *Fires from Nuclear Weapons*, Pacific-Sierra Research Corporation, Report 1881, March 1989 (in press as Defense Nuclear Agency Effects Manual, EM-1, Chapter 16).

Small, R. D., J. Blair, and K. E. Heikes, *Early Smoke Plume and Cloud Formation by Large Area Fires*, Pacific-Sierra Research Corporation, Report 1728, May 1987.

Small, R. D., and K. E. Heikes, "Early Cloud Formation by Large Area Fires," *J. Appl. Meteorol.*, Vol. 27, No. 5, May 1988, pp. 654-663.

Small, R. D., and K. E. Heikes, "Target Area Smoke, Clouds, and Turbulence," *Proceedings of the Smoke/Obscurants Symposium XIII*, Laurel, MD, April 25-27, 1989, Unclassfied Section, Vol. II, pp. 541-555.

Small, R. D., and D. A. Larson, "Velocity Fields Generated by Large Fires," *Israel J. Technol.*, Vol. 22, pp. 173-186, 1984/5.

Smith, R. K., "Radiation Effects on Large Fire Plumes," *Eleventh International Symposium on Combustion*, The Combustion Institute, Pittsburgh, PA, pp. 507-515, 1967.

Turner, J. S., *Buoyancy Effects in Fluids*, Cambridge University Press, Cambridge, England, 1973.

Weihs, D., and R. D. Small, *Interactions and Spreading of Adjacent Large-Area Fires*, Pacific-Sierra Research Corporation, Note 719, March 1986; also DNA-TR-86-214, Defense Nuclear Agency, Washington, DC.

Westphal, D. L., O. B. Toon, and W. R. McKie, "An Investigation of the Dynamical and Radiative Effects of Regional-Scale Smoke Plumes," Technical paper presented at the Defense Nuclear Agency *Global Effects Review Meeting*, April 19-21, 1988, Vol. II, July 1988, pp. 244-277.

DISTRIBUTION LIST

DNA-TR-89-20-V5

DEPARTMENT OF DEFENSE

DEFENSE INTELLIGENCE AGENCY
ATTN: DB-6
ATTN: DB-6E2
ATTN: WDB-4CR

DEFENSE NUCLEAR AGENCY
ATTN: OPNS
ATTN: RAAE K SCHWARTZ
2 CYS ATTN: RARP
ATTN: SPWE
2 CYS ATTN: TDTR
2 CYS ATTN: TITL

DEFENSE TECHNICAL INFORMATION CENTER
2 CYS ATTN: DTIC/FDAB

FIELD COMMAND DEFENSE NUCLEAR AGENCY
ATTN: FCNM
2 CYS ATTN: FCTT W SUMMA

THE JOINT STAFF
ATTN: JKCS

DEPARTMENT OF THE AIR FORCE

STRATEGIC AIR COMMAND/XRFS
ATTN: XRFS

DEPARTMENT OF ENERGY

LAWRENCE LIVERMORE NATIONAL LAB
ATTN: J PENNER
ATTN: L-442 J BACKOVSKY
ATTN: L-81 R PERRETT
ATTN: M MACCRACKEN

LOS ALAMOS NATIONAL LABORATORY
ATTN: M GILLESPIE

SANDIA NATIONAL LABORATORIES
ATTN: B ZAK ORG 6321

OTHER GOVERNMENT

FEDERAL EMERGENCY MANAGEMENT AGENCY
ATTN: OFC OF CIVIL DEFENSE J F JACOBS
ATTN: P BRYANT

NASA
ATTN: O TOON
ATTN: T ACKERMAN

NATIONAL CENTER ATMOSPHERIC RESEARCH
ATTN: S SCHNEIDER

NATIONAL INSTITUTE OF STANDARDS & TECHNOLOGY
ATTN: H BAUM
ATTN: R LEVINE

OFFICE OF SCIENCE AND TECH POLICY
ATTN: MAJ S HARRISON

DEPARTMENT OF DEFENSE CONTRACTORS

DESERT RESEARCH INSTITUTE
ATTN: J HUDSON

INSTITUTE FOR DEFENSE ANALYSES
ATTN: E BAUER

KAMAN SCIENCES CORP
ATTN: DASIAC

KAMAN SCIENCES CORPORATION
ATTN: DASIAC

MISSION RESEARCH CORP
ATTN: G MCCARTOR

PACIFIC-SIERRA RESEARCH CORP
2 CYS ATTN: D WEIHS
ATTN: H BRODE
2 CYS ATTN: R SMALL

SCIENCE APPLICATIONS INTL CORP
ATTN: L HUNT

SCIENCE APPLICATIONS INTL CORP
ATTN: D BACON
ATTN: J COCKAYNE
ATTN: J MCGAHAN

STAN MARTIN AND ASSOCIATES
ATTN: S B MARTIN
ATTN: S MARTIN

SWETL, INC
ATTN: T Y PALMER

TRW INC
ATTN: F FENDELL

UNIVERSITY OF NEW MEXICO
ATTN: H GLOVER

UNIVERSITY OF WASHINGTON
ATTN: L RADKE